

Pathfinding with the Old Breed: Using old clusters of the Milky Way for Galactic Tracing

OWEN JOHNSON ¹

¹*School of Physics, University College Dublin, Ireland*

ABSTRACT

Open clusters have been long used as stellar laboratories, and galactic tracers in this study both are used in tandem to investigate the distribution of old (> 1000 Myr) open clusters in a milky way. UB photometric data were collected for Berkeley 28, Bochum 2, NGC 2124 and NGC 2155. Each cluster's population was determined using Gaia data and parameterised using MIST and DSEP isochrones. Along with classification based on the Trumpler scheme and cataloguing of the stellar population. These clusters were combined with 266 open clusters from newly available catalogues. It was found that there is an underabundance of old open clusters within the inner galactic disk of the Milky Way despite production outweighing disruptive dynamical forces in the galaxy. It is shown that there is no direct correlation between cluster age and galactic position. Indicating sprawling embedment of older clusters throughout the milky way is due to a layered relationship between internal cluster dynamics and the disk environment. It is deemed that an underabundance of old clusters is due to dispersion due to destructive interactions and misrepresentation due to observational selection. With the old breed of open clusters found to be inflating the galactic disk.

Keywords: Open Clusters — Galactic Tracing — Galactic Disk — MIST Isochrone Fitting

*This work is dedicated to my mentor and my friend
Noel White, (1951-2021).*

1. INTRODUCTION

Open clusters have been shown to be an integral part of the astronomer's toolbox, readily lending themselves as stellar laboratories. Open clusters are classified as a group of stars around the same age and loosely bound through mutual gravitation.

Their similar age allows for in-depth observation of the stellar evolution. Through this, many attributes of the stellar population can be inferred. As clusters span age ranges from a couple of Myr to Gyrs, many have been present since the formation of the disk itself. Through this, if clusters of varying ages are examined, it is possible to trace the evolution of the milky way.

Mapping the milky way has always been difficult, given the vantage point it can be observed from. This makes it quite challenging to appreciate the shape and dimensions of the milky way. Some of the pioneering studies, such as ?? and ? first outline the use of open clusters to map the galaxy. Following with studies like ? which pathed the spiral arms of the milky way using open clusters and numerous studies by ? which explore

the evolution of the galaxies scale height.

To more recent studies such as ?. Which use young open clusters to predict shape evolution of the galaxy, by analysing to longitudinal distribution of young clusters to predict reflect on areas of star formation and presence of spiral arms.

While the precision and accuracy of cluster age estimates are tied to the quality of the observational data and theoretical models, the process of estimating cluster age through the use of colour-magnitude diagrams is relatively straightforward and has been shown to be tried and true. Even early open cluster catalogues like ? included distance estimates, while more recent catalogues like ? have provided other parameters such as age, metallicity and excess colour. Furthermore, with the second data release from Gaia (GDR2; ?). presents the most in-depth all-sky astrometric and photometric study to date.

This increase in available data has allowed for the characterisation of open clusters on mass adding to catalogues such as WEBDA. Determination of all open clusters identified by Gaia is an ongoing task and is being automated using modern techniques and machine

learning as shown in studies by ? and ?.

This study used the 1.25 m optical telescope at the Calar Alto Observatory (CAHA) to observe four open clusters from the WEBDA catalogue. The aim of this work was to classify the four observed clusters and infer details of each cluster. Then use this observational cluster classification in tandem with other open clusters from the WEBDA catalogue to trace the paths of clusters in the galactic disk, studying both its structure and evolution.

2. OBSERVATIONS

This study observed 4 open-clusters from the WEBDA database on the night of March 10th 2022. Each cluster was observed using B and V filters in the Johnson Cousins' UBV system. The average observation time for each cluster was X with image calibration and reduction carried out.

2.1. Target Selection Strategy

For this work it was important for the sample to observe clusters grouped at a similar area of the galactic disk (see. ??) at varying estimated cluster ages, with each group containing an old (> 1000 Myr), young (< 100 Myr) and one intermediate cluster. In grouping the targets like this it would allow for comparison between galactic position of and varied age, giving the most to the small quantity of clusters analysed. The observed targets are listed in ??. A further six open clusters from the WEBDA catalog are also analysed to add to the sample size of clusters analysed and classified by the methods of this work. The six cluster were intially proposed for observation but not-observed due to poor conditions during the observation period.

2.2. Photometry

Photometric analysis was carried out by first using DA0StarFinder with a FWHM chosen taken as the average of moderate sources to favour an array of sources. Aperture photometry performed as standard. To try make the most of the detected sources an trial apertures were taken on each source locating the aperture that corresponded to the highest SNR value. The aperture for each max SNR value was noted, with the final used aperture value used was taken to be the mean value of all sources apertures that did not exceed a SNR value of 50 or greater. Much like the choice around the FWHM value this choice was used to optimise the magnitudes attained for all detected sources.

2.2.1. Magnitude Calibration

The instrumental magnitude was calibrated to the real magnitude using 9th data release of the AAVSO Photometric All Sky Survey (APASS9). Each source was queried to the APASS9 catalog if a source in the catalog was within 3 pixels (1.806 arcsec) of source centroid position the query was considered a match and respective real (M_{real}) and instrumental magnitudes ($M_{\text{inst.}}$) saved.

A linear relationship was formed between M_{real} and $M_{\text{inst.}}$ and used for instrumental conversion.

2.2.2. Error on Magnitude

As this study also catalogs 4 clusters it was important to quantify error on each of collected magnitude. For this §6 of ? was followed closely. This allowed for errors on $M_{\text{inst.}}$ to be ascribed to M_{real} using the derivative and added to quadrature in $M_{\text{inst.}}$. Then using the full covariance matrix for propagation through a fitted function gave an error for converted magnitudes, taking both the APASS error and the error given by SNR ($\Delta M \sim 1/\text{SNR}$)

$$\sigma_{M_{\text{conv.}}} = \sqrt{M_{\text{inst.}}^2 \sigma_m^2 + \sigma_c^2 + 2M_{\text{inst.}} \sigma_{mc}^2} \quad (1)$$

Where $M_{\text{conv.}}$ is the converted magnitude and m and c are the slope and constant the linear fit. The covariance cross-term σ_{mc} was considered negligible due to the internal precision of `numpy.float`.

3. POPULATION DETERMINATION

The main obstacle in studying open clusters is determining the validity of a sources membership in the population. This problem can often be negated by using spatial distribution to try determine which stars pose likely candidates. This method has seen some success as seen in studies such as ? and also in the study of globular clusters as recently shown by ?. This method falls short when dealing with clusters that have a moderate to low degree of concentration and no discernable shape as with the majority of open clusters.

The field of determining cluster populations is one that sees frequent studies but there is no one particular method widely accepted. One promising study is ? which approaches the problem by basis of photometric membership using Bayesian statistics which would remove the reliance on supplementary astrometric or spectroscopic data.

However, this study incorporates the use of Gaia's second data release.

3.1. Using Gaia

Table 1. List of analysed targets.

Target Cluster	RA (J2000)	DEC (J2000)	WEBDA Study
	hh:mm:ss	deg:mm:ss	
Berkeley 28	06:52:12	02:56:00	?
Bochum 2	06:48:54	00:23:00	?
NGC2324	07:04:07	01:02:42	?
NGC2355	07:16:59	13:45:00	?
<i>Proposed Open Clusters</i>			
Berkeley 20	05:33:00	00:13:00	?
Berkeley 34	07:00:24	-00:15:00	?
King 1	00:22:04	64:22:50	?
King 15	00:32:54	61:52:00	?
NGC 2129	06:00:41	23:19:06	?
Stock 18	00:01:37	64:37:30	?

NOTE—Above details the targets analysed throughout this work. The first four targets were observed at CAHA. With the following six grouped as the proposed clusters. The associated WEBDA study used for supplementation is also listed.

This study takes full advantage of Gaia’s DR2. Each observed cluster is queried collecting entries for stars within 10 arcmins of the cluster center. Each returned entry then was filtered based on the associated error on the G-band mean magnitude with values of < 0.01 accepted.

A hierarchical density based scan (HDBSCAN) was then used on the parallactic data to determine possible members of the population.

A density based scans or DBSCAN is an algorithm first brought coined by ?. DBSCAN works given two parameters a linking length, ϵ and minimum neighbourhood point. An illustration of this can be seen in ??, where a point is consider a neighbour if it falls within the linking distance of another point and is then considered a set once the defined threshold for cluster size is met.

A HDBSCAN is a decendant of DBSCAN created by ?. In the case of HDBSCAN there is no dependency on linking (ϵ), instead pruning nodes that do not meet the star population threshold and re-analysing the ones that do.

The benefits of using parrallax compared to photometric data can be seen in ??. Where a usually DBSCAN or HDBSCAN would remove stars that are off the main sequence the parrallax retains the non-mainsequence population. As this performs on a hierarchical basis the probability of a star being part of a cluster is related to the ‘distance’ between the first (‘birth’) cluster and the last cluster (‘death’). The persistence of a cluster is expressed as $\lambda = \frac{1}{\text{distance}}$, where distance is the distance from the core cluster. The persistence of birth and death is then λ_{birth} and λ_{death} respectively.

The stability of a classified cluster is then

$$\text{stability} = \sum_{p \in \text{cluster}} (\lambda_p - \lambda_{\text{birth}}) \quad (2)$$

The probability of a point in a cluster is then classified as the normalised corresponding stability. The results of this classification can be found in ??. The uncertainty on the population is taken proportion of the population that had 80% or less membership probability. With the expected population taken from ? and in the case of Bochum 2 taken from ?.

Table 2. Results of Gaia population classification.

Target	Population	Study Population
Berkeley 28	79 ± 17	53
Bochum 2	110 ± 13	110
NCG 2324	251 ± 26	242
NGC 2355	139 ± 128	261

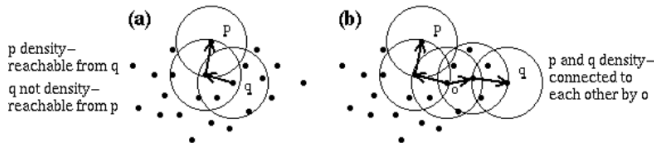


Figure 1. Example of DBSCAN selection showing how points are linked together. Figure courtesy of ?.

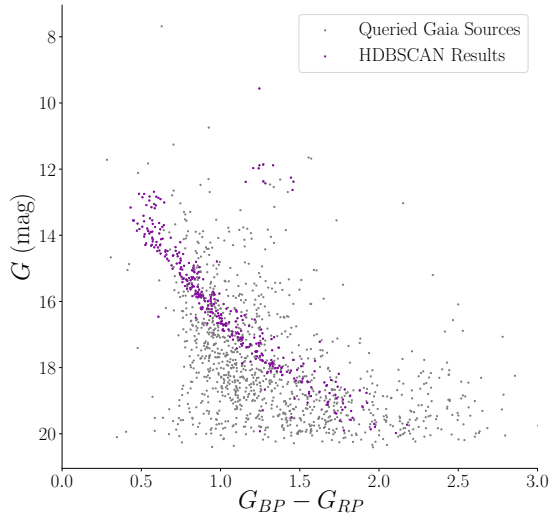


Figure 2. Stellar population determined for NGC 2355 using Gaia parallax data and HDBSCAN method.

Determining the population through the use of HDBSCANs and Gaia provided promising results. Each cluster responded to the filtering with the underestimations seen in NGC 2123 impart due from stars with a magnitude of 19 or greater. However the calculated probabilities had varying results in quantifying and uncertainty. For the more sparsely populated cluster such as Berkeley 28, Bochum 2 and NGC 2324 the probabilities returned a mean membership rate of 89%, 92%, and 95% respectively. While these estimations appear adequate and are in line with the ranges shown for these clusters in similar studies (????) the population of each cluster should be around a 30% underestimation given the distribution of brightness in each cluster.

4. DETERMINING CLUSTER PARAMETERS

Following the cluster population analysis the next step is fitting parameters to the set of observed and proposed open-clusters.

4.1. Isochrones

4.1.1. Detailing MIST

The isochrones generated for use in this study were created using the MESA Isochrones and Stellar tracks (MIST; ?) from the Modules for Experiments in Stellar Astrophysics (MESA; ?). MIST uses the Sun as a basis for its chemical compositions, with solar abundances modelled by ? with $Z_{\odot} = 0.014$. MIST takes hot wind-driven mass-loss from ?, cooled dust driven mass loss from ? and ? for any mass loss in the helium star

phase. With convection boundaries modelled after ? and convection overshooting modelled using ?.

4.1.2. Using MIST

The choice of using MIST was due to its recent creation compared to WEBDA used isochrones (Padova & Geneva) and also its ease of interpolation oppose to other commonly used isochrones like PARSEC. A detailed comparative studies of popular modern isochrones is carried out by ?.

Interpolation and plotting was carried out using a forked version of the *isochrones* package created by ?. *isochrones* possessed a high functioning front end for accessing MIST isochrones from the Johnson UBVI system and plotting with minimal turnaround time. This allowed for quick incremental change in the parameters generating isochrones making the process for incrementally fitting isochrones less cumbersome.

4.2. Isochrone Results

Isochrone fitting was carried out on 10 clusters as listed in ??. The 4 observed clusters, Berkeley 28, Bochum 2, NGC 2324 and NGC 2355 along with the 6 proposed clusters. The resultant parameters from these fits can be seen in ??.

Each cluster's parameters were compared to both their corresponding WEBDA study and ? to compare attain value. Of the 4 observed clusters the 2 youngest clusters Bochum 2 (Bo 2) and Berkeley 28 (Be 28) did not show any discernable main sequence. This can be clearly seen in ??

4.3. Goodness of Fit

Fitting isochrones in itself can be an unwieldy task and often difficult to quantify the 'goodness' of fit. In this case the isochrone was first fitted by varying values of colour to find the extinction in the V band using the following expression as per (?, pg. 237).

$$A_v = 3.1 E(B - V) \quad (3)$$

Distance was then determined taking into account the value for extinction. Both age and metallicity were determined by fitting various incremental parameters by eye and taken the 'best' fit as the parameters value. The errors were taken to be the limits where the parameters had argument for being a 'good' fit. While not a quantitative or rigorous method for justifying a data fit it has historically provided results with an adequate degree of confidence. The release of GDR2 has prompted a new wave of studies developing means of attaining a tangible goodness of fit for modern isochrones. ? has

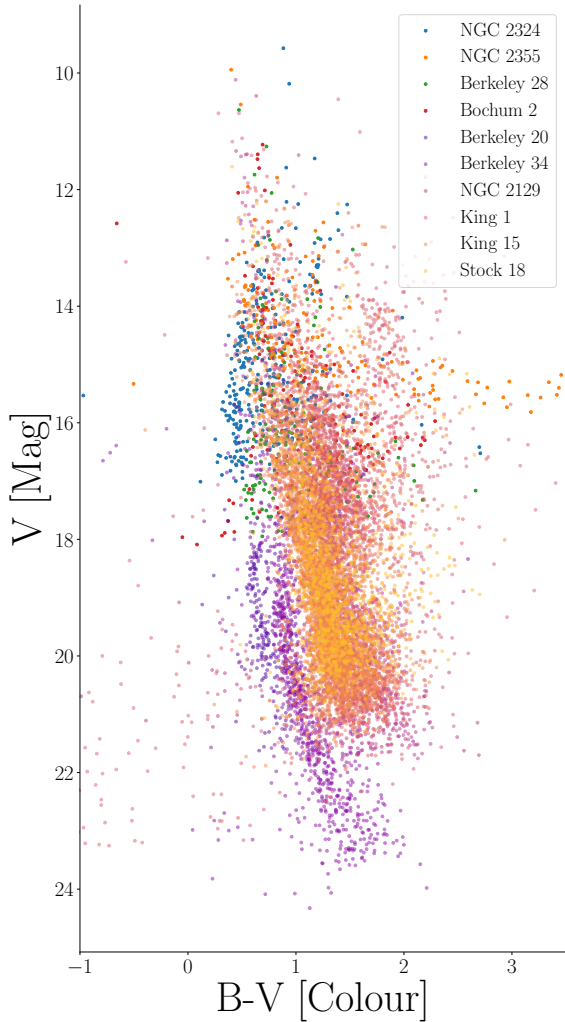


Figure 3. Overall CMD plot of all stars analysed in this study. This illustrates homogeneity of the stellar population distributed along the main-sequence. Each colour representing an open cluster.

coined a promising method of Mahalanobis distances of stellar data points to plotted isochrones and mask resultant synthetic CMDs with χ^2 distributions to fit to Gaia samples as a mean of seeing if a fit is good.

5. CLASSIFICATION

5.1. Open Cluster Classification Scheme

As open clusters span many different distributions in both density, size and stellar constituents. Open clusters can contain large stellar agglomerations to just a handful of stars. While classification systems can vary based on the context of the study the scheme coined by ? sees prominent use.

This scheme classifies cluster based on three factors of the stellar population. a) their range of brightness, b) degree of concentration and c) star population in the cluster. The details of this classification scheme can be seen in ?. In this study each observed target is classified based on this scheme.

5.2. Classification Results

Each cluster was classified based on the distribution of V magnitude which can be seen on the y-axis of both ?? and ?. With the concentration of each cluster based on distribution of confirmed stars from the cluster's center.

The results of each classification can be seen in ?. Each cluster was deemed to match ? and CITE JANES

6. SUPPLEMENTARY DATA FOR TRACING

This study directly uses 260 clusters cataloged by ? to aid the observational sample size. This study also uses a 269 cluster catalog by ? to use as comparison to determined observational parameters. When searching for studies to compliment this work use Gaia's second data release (DR2) was given preference. The reason for the use of supplementary data was to provide a more varying survey of the galactic disk. The first data set implemented was 269 clusters analysed and catalogued by ?. This dataset contains large sample of clusters analysed from Gaia DR2, with each of the clusters containing a high degree homogeneity among the stellar population. The cluster populations were determined using Bayesian methods of statistics along with DR2 astrometric data. In doing this the probability of each star being a member of each cluster was 70% or greater. The parameters of each cluster was found using PARSEC isochrones (?). This data set worked well to fill out a sample size in the galactic disk as seen in ?. Although this survey contained a good amount of clusters with varying age it lacked a lot of ancient clusters of the milky way. To supplement this gap 260 old clusters from ? were used. This study used a neural network trained on high accuracy data sets to estimate cluster parameters using GDR2 parallax values and photometry ($G \leq 18$).

6.1. Cataloging

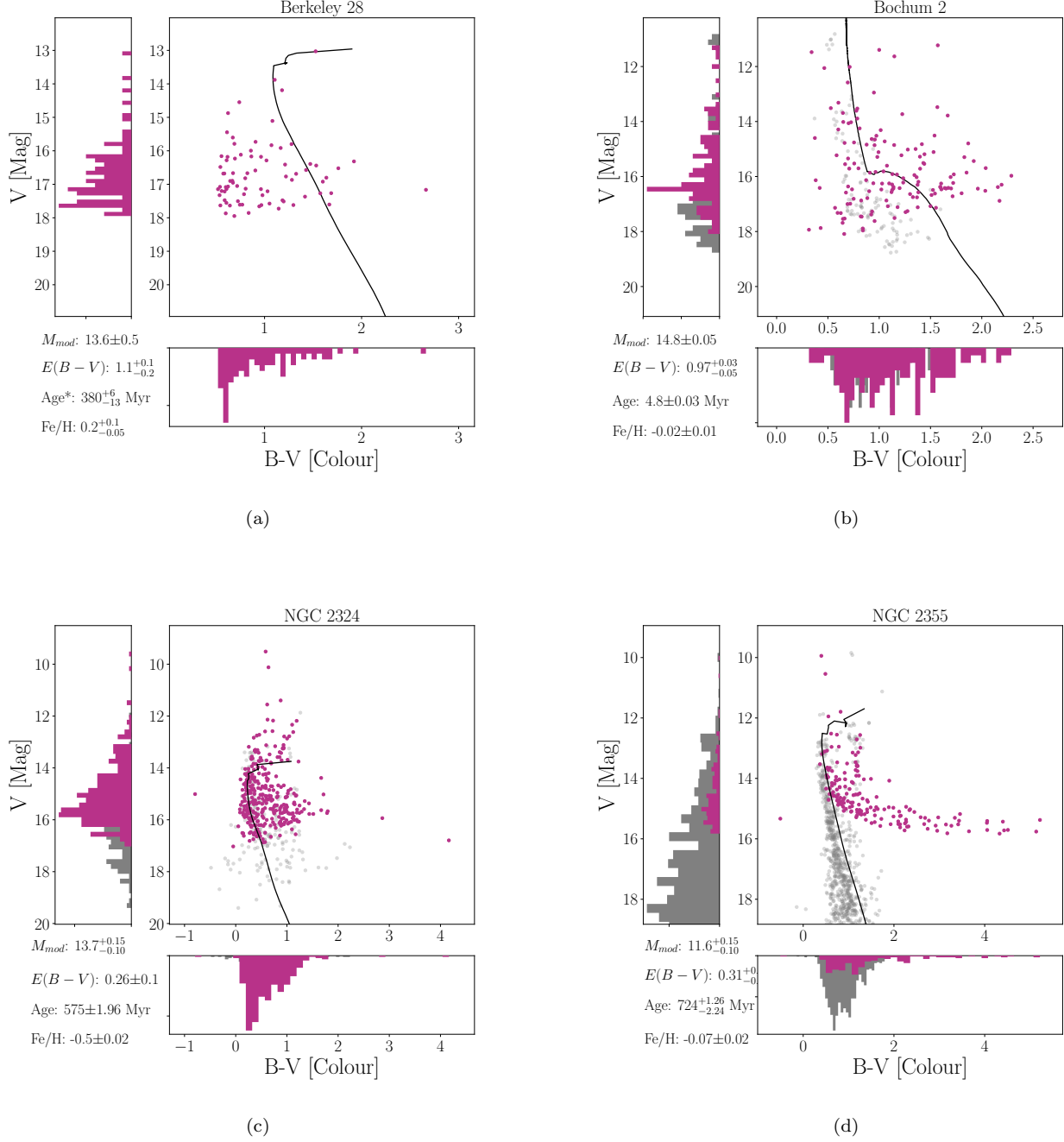
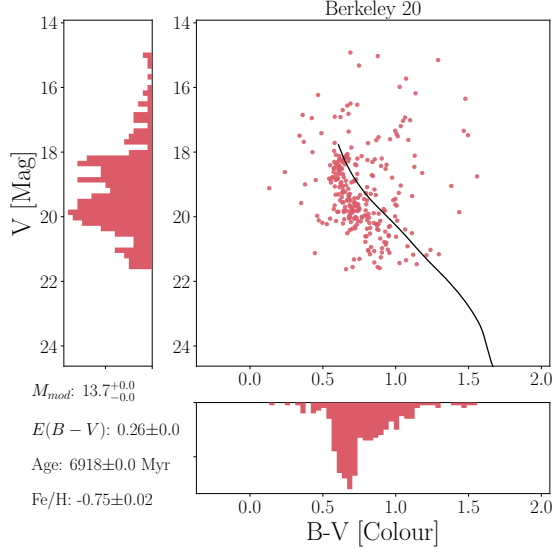
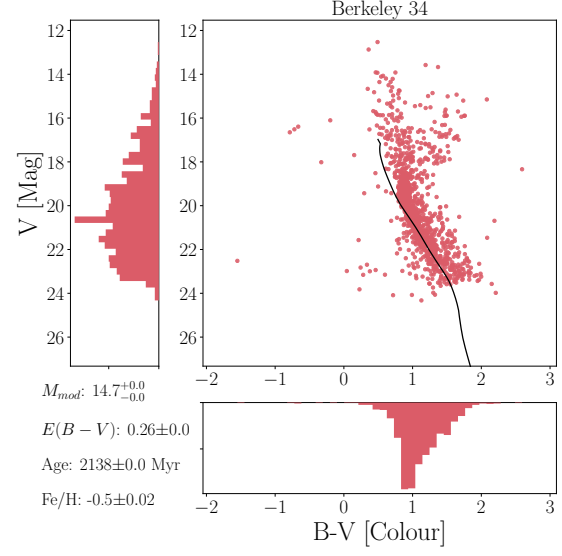


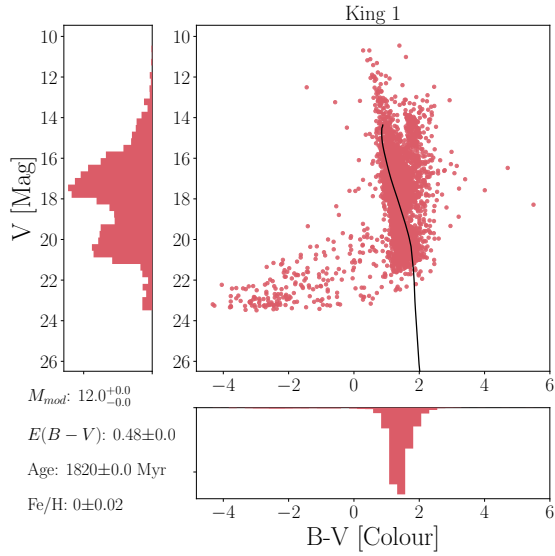
Figure 4. Colour magnitude diagrams fitted to MIST isochrones of observational data with complementary WEBDA data plotted in grey. Histogram on each the x and y axis represent distribution of colour and magnitude respectively.



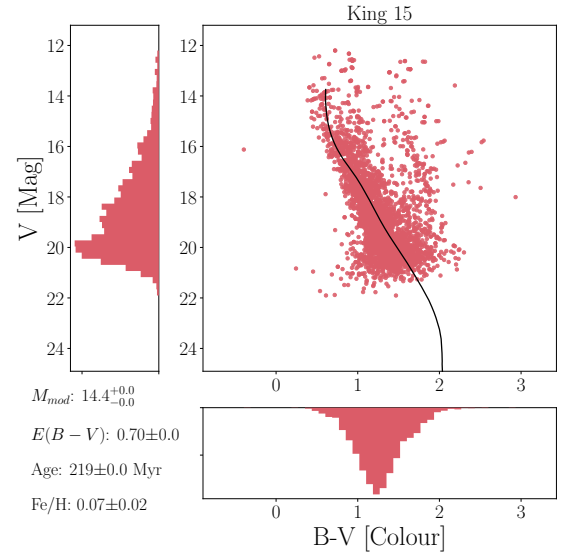
(a)



(b)



(c)



(d)

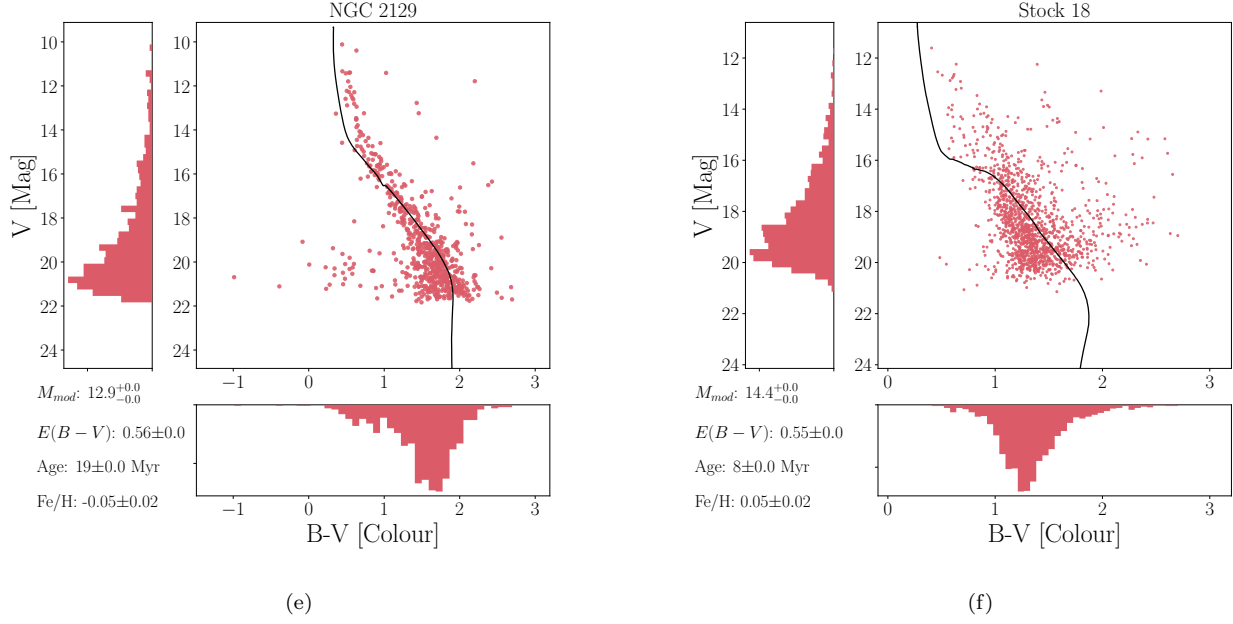


Figure 5. Colour magnitude diagrams fitted to MIST isochrones of observational data with complementary WEBDA data plotted in grey. Histogram on each the x and y axis represent distribution of colour and magnitude respectively.

Table 3. Cluster parameters.

Cluster	Age		Distance		Colour		Metalicity		Extinction	
	Myr		M_{V_0}		$E(B - V)$		Fe/H		A_v	
	Obs.	Study	Obs.	Study	Obs.	Study	Obs.	Study	Obs.	Study
Berkeley 28	63^{+6}_{-13}		11.9 ± 0.5		$0.1^{+0.05}_{-0.05}$		$0.2^{+0.1}_{-0.05}$		0.31 ± 0.16	a
Bochum 2	5 ± 0.2		13.2 ± 0.4		0.64 ± 0.1		$-0.02^{+0.005}_{-0.005}$		1.98 ± 0.31	a
NGC 2324	427 ± 0.5		13.2 ± 0.05		0.26 ± 0.03		-0.52 ± 0.07		0.81 ± 0.09	
NGC 2355	$676^{+3.44}_{-1.64}$		$11.6^{+0.06}_{-0.05}$		$0.31^{+0.06}_{-0.03}$		-0.07 ± 0.02		0.96 ± 0.12	
Berkeley 20	6026^{+12}_{-12}	5000	$14.4^{+0.2}_{-0.3}$	15.1 ± 0.8	0.09 ± 0.03	0.13	-0.35 ± 0.05	-0.75	0.28 ± 0.09	0.403
Berkeley 34	2239^{+24}_{-24}		$14.7^{+0.3}_{-0.1}$		$0.5^{+0.1}_{-0.1}$		0.02 ± 0.005		1.55 ± 1.33	a
King 1	2455^{+52}_{-52}		$11.2^{+0.5}_{-0.5}$							a
King 15										a
NGC 2129										a
Stock 18										a

NOTE—The above table contains the determined value for both observed and proposed clusters along with the relevant WEBDA collected data by authors outline in ??.

Table 4. Trumpler classification scheme.

Range of Brightness (a)	Degree of Concentration (b)	Cluster Population (c)
1 - Majority of stellar objects show similar brightness.	I - Strong central concentration (Detached)	p - Poor ($n < 50$)
2 - Moderate brightness ranges between stellar objects.	II - Little central concentration (Detached)	m - Medium ($50 < n < 100$)
3 - Both bright and faint stellar objects	III - No discernible concentration IV - Clusters not well detached (Strong field concentration)	r - Rich ($n > 100$)

NOTE—Where n denotes the amount of the stellar population in a given cluster. For example Pleiades is a I3rn cluster and Hyades is a II3m cluster. Where the 'n' flag on a classification relates if the cluster shows nebulosity.

Stars that were confirmed as part of the population have been cataloged with their respective parameters and can be found in X.

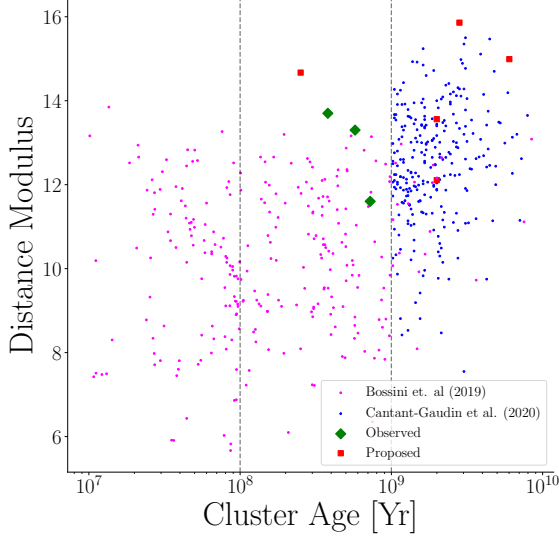


Figure 6. Distance against the log age of both observed targets, proposed targets and supplementary targets. This plot illustrates the gap of old clusters from ?’s data fills.

7. GALACTIC TRACING

Following the classification of the four observed clusters and parameterising of the 10 clusters both proposed. They’re age and location was used to make an enquiry into the present shape of the galactic disk. Here ? sample of old open clusters is used fully. A preliminary caveat is the use of the term ‘inner-disk’. For this work as with similar studies the inner-disk is taken to be clusters that fall within a galacto-centric distance smaller than the Sun. This value¹ is taken to be 8180 ± 35 pc given by ?.

7.1. Distribution of Old Clusters

The sample size collected for this study includes old open clusters from across the galactic disk at varying distances as seen in ?? and ?. Plotting the distribution of these clusters can be seen in ?. The immediate takeaway from this depiction is the lack of older open clusters within the innerdisk. Out of the

265 old clusters present only 62 (23.8%) reside within the inner galactic disk. Moreover looking at the distribution of ages for as a function of both galocentric radius

7.2. ** Reasons for Underabundance

Trying to determine a reason for the underabundance seen in older open cluster in the galactic inner disk has been a question since the start of using open-clusters in galactic tracing. ? assumed uniform star formation in the disk and initially deemed it to be a case of extrapolation of younger clusters as open cluster which were much less prominent by nature.

The most intuitive explanation would that over time both gravitational pull and destructive tidal forces would cause any open cluster to be pulled apart and dissipate into other surrounding objects through a long term interactions.

? derives a model for the evaporation of stars from open clusters based on mass distribution of opencluster and applies the model to the Pleiades predicting that all opencluster eventually dissipate. More recently ? confirmed the decline in stellar population in 6 open clusters. This distribution is based on dynamic simulations of age, limiting radius, stellar mass, and velocity dispersion. Looking outside the realms of internal dynamics in the cluster causing dispersion there is also interactions with other objects in the galactic disk causing an acceleration of cluster degeneracy. The primary suspect in these disruptive interactions is massive dust cloud in the galactic core as first noted by ?. Here it was stated that for a cluster of a mean density of M_{\odot}/pc^3 the dispersion time would be ~ 200 Myr. Such that lower mass clusters would disperse at a much faster rate.

While the precessing arguments have both logic and evidential basis for these findings and open cluster do increasingly disperse with time. There are few contradictory points of interest.

7.3. Relating Cluster Age to Galactic Position

The interesting consideration is that despite the internal and external interactions discussed in the previous section there is still a appreciable amount of older clusters close to the galactic disk. Berkeley 17 (10 Gyr) and Collinder 261 (8 Gyr) are both within 200 pc of the plane. As ? discusses since the release of GDR2 confirmation of 9 old clusters² within $R_{GC} < 6500$ pc. Small parallax coupled with sparse CMDs as illustrated by Be 28 indicate that there could be more clusters located deeper in the disk within this region, but dif-

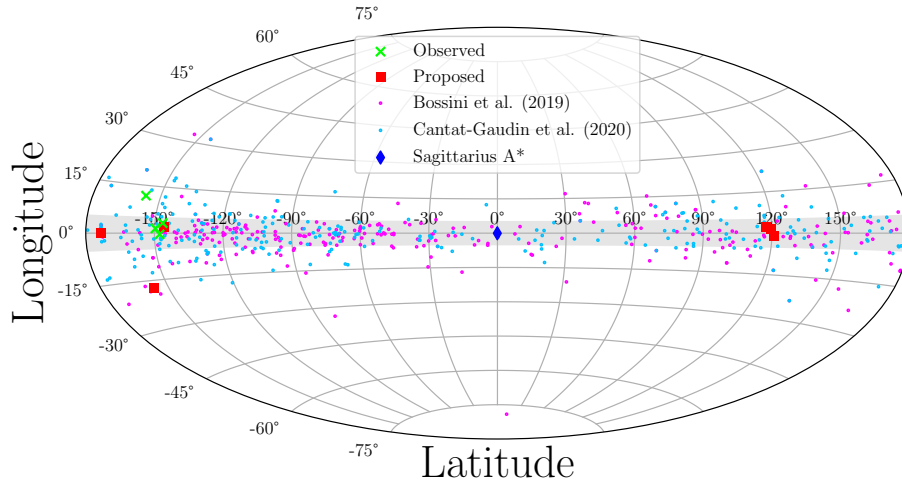
¹ Currently the most accurate accepted value for solar distance to Sagittarius A*

² NGC 6005, NGC 6583, UBC 307, UBC 310, UBC 339, LP 866, UFMG 2, Ruprecht 134, and Teutsch 84

Table 5. Results of Trumpler classification on observed targets.

Target	ΔV_{mag}	ΔB_{mag}	σ_c	Population n
Berkeley 28				79 ± 17 m
Bochum 2				110 ± 13 r
NGC2324	12	12	12	251 ± 26 r
NGC2355				139 ± 128 r

NOTE—Where n denotes the amounts the stellar population in a given cluster. For example Pleiades is a I3rn cluster and Hyades is a II3m cluster. Where the 'n' flag on a classification relates if the cluster shows nebulosity.

**Figure 7.** Aitoff projection of targets in terms of galactic co-ordinates, longitude (l) and latitude (b). Targets observed at CAHA are observed in X, the original proposal targets shown in X and studies by ? and

ficulty inferring thier parameters prevents meaningful estimates of distance.

While the first large scale catalogs of open clusters by ? and ? suggest that destructive forces are too efficient to relate to the amount of older clusters currently seen.

?? shows no clear relationship between the age of a given cluster and its galocentric distance. As shown by ?? most of the old clusters lay outside the innerdisk with 4 of the clusters under 1000 Myr also situated outside the innerdisk. When looking at ?? there is also no clear relationship between age and cluster presence in the bulge. The extreme outliers of clusters like Be 20 could be residual formation from an interaction of more populas clusters near the bulge.

Given these factors it is likely that the relationship between cluster age and position in the galactic plane is a nuanced relationship between inherent cluster prop-

erties, internal dynamics and the overall enviroment in the galaxy.

An extension to this study would be to use GDR2 to investigate the orbits of old and ancient open clusters. It has been shown in studies X and X that older open clusters adhere to extensive ellpitcal orbits. If these orbits were simulated on a large enough time-scale it could show a migration pattern into the inner-disk. It would also be worth-while to further explore the internal dynamics of the cluster, finding a relation between intial-mass of older open clusters and the strength of their gravatiational bounds.

7.4. Galatic Evolution

As there is a substatial amount of older clusters found throughout the disk with evidence of a substatial survival rates. The disk indicates a thincking of the galactic disk

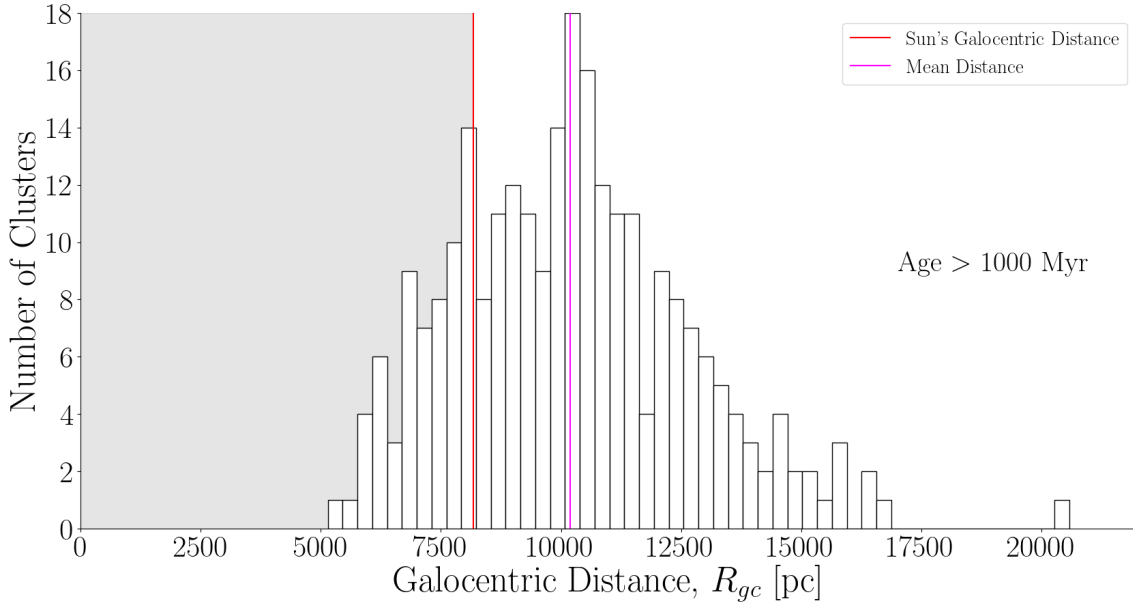


Figure 8. Distribution of old clusters according to galocentric distance. This sample includes 10 clusters of this work and 260 old open clusters from ?. The inner disk region is shaded.

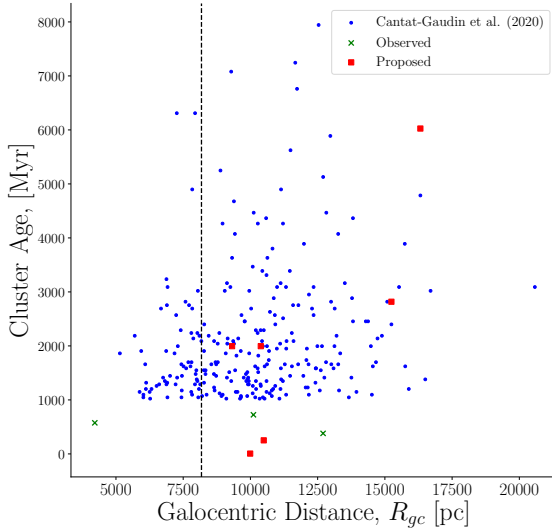


Figure 9. Plot of cluster age against distance galocentric distance, R_{gc}

with increased galocentric distance. The excursion of old open clusters to larger galocentric distances away from disruptive appears to be highly assymmetric. There also could be observational selction at play as previously stated with asterism and difficulty differentating older clusters from concertrated areas in the disk. These findings are also echoed in ?.

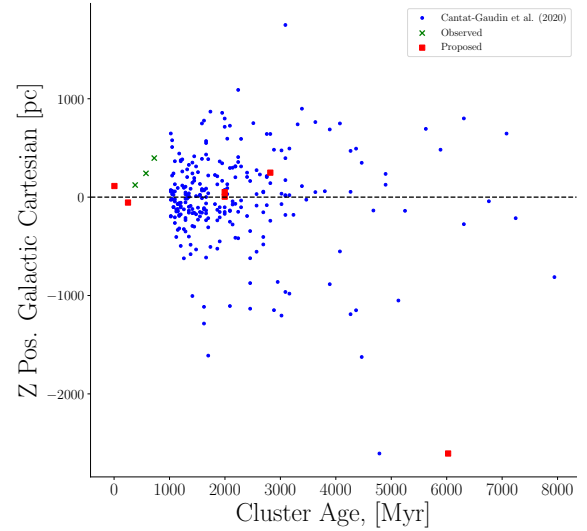


Figure 10. Plot of cluster age against galactic cartesian co-ordinates in the z-direction, Z .

8. CONCLUSIONS

This study collect UV data on four clusters from the WEBDA catalog. Each observed cluster was classified based on exclusively Gaia's second data release through hierarchical density based scanning. Each cluserter was characterised using MIST isochrones and supplemented

using DSEP isochrones. The observed clusters were then classified based on the Trumpler classification scheme and cataloged.

Additionally a further 6 clusters of interest were also characterised using MIST isochrones. Each cluster showed resultant parameters that fell within expected range of either their relevant WEBDA study or entry in the collected supplementary data. Any large invariance due to the lack of definition on the main-sequence (Be 28 and Bo 2) and smaller variance expected due to the fitting of modern isochrones.

9. THIRD PARTY SOFTWARE AND CATALOGS

This work made use of a variety of software suites and python modules. [Ginga](#) was used as the primary image viewer and used as reference when performing photometry.

All data and processing files can be found on the author's [GitHub](#).

ACKNOWLEDGMENTS

I would like to give my thanks to Dr Antonio Martin-Carillo for his patience, warmth and depth throughout this project. He made this project an absolute joy from start to finish. I want to give a special thanks to Camin Mac Cionna for his marvellous code, coffee and 'career' advice, to my open cluster partner in crime, Eoin Fitzpatrick, for making my exploration of the universe a little less lonely and to Sean J. Brennan for the wise insights and advice in cycling and astrophysics a-like. Furthermore, I would like to thank my peers for making the last four years of learning about the cosmos the best experience I've ever had. I wish them every luck and success in their future careers.

To A-a-ron, Ben, Ciara, Cian, Hugh, Joe, Laura, Sharon, and Tiernan, thank you for taking care of me for the past few years. Your friendship is both invaluable and necessary.

Finally, to my family, for their unwavering support and help in the pursuit of my dreams always. Thank you for making all of this possible.

APPENDIX

A. STELLAR CATALOGS

Table 6. Stellar catalog for NGC 2324.

<i>no.</i>	RA J2000	DEC J2000	B Magnitude	V Magnitude	BV Magnitude
<i>Population Size: n = 251</i>					
1	106.0320	1.0263	16.979 ± 0.2136	16.222 ± 0.1053	-0.308 ± 0.2213
2	105.9987	1.0177	17.434 ± 0.2181	16.054 ± 0.1044	0.314 ± 0.2252
3	106.0556	1.0286	17.084 ± 0.2145	16.007 ± 0.1042	0.011 ± 0.2216
4	106.0382	1.0512	17.094 ± 0.2146	15.944 ± 0.1039	0.084 ± 0.2215
5	105.9826	1.0289	17.342 ± 0.2171	15.849 ± 0.1035	0.428 ± 0.2238
6	106.0143	1.0555	17.057 ± 0.2142	15.835 ± 0.1034	0.156 ± 0.2210
7	106.0161	1.0613	17.110 ± 0.2147	15.825 ± 0.1034	0.219 ± 0.2214
8	106.0291	1.0476	16.778 ± 0.2122	15.814 ± 0.1033	-0.102 ± 0.2190
9	106.0309	1.0594	16.918 ± 0.2131	15.761 ± 0.1031	0.090 ± 0.2198
10	106.0442	1.0013	16.991 ± 0.2137	15.721 ± 0.1029	0.204 ± 0.2202
11	106.0495	1.0284	16.669 ± 0.2116	15.717 ± 0.1029	-0.114 ± 0.2182
12	106.0369	1.0464	16.785 ± 0.2122	15.707 ± 0.1029	0.012 ± 0.2188
13	105.9968	1.0264	16.638 ± 0.2114	15.703 ± 0.1029	-0.131 ± 0.2180
14	105.9931	1.0016	17.073 ± 0.2144	15.692 ± 0.1028	0.315 ± 0.2209
15	106.0407	1.0536	16.925 ± 0.2132	15.667 ± 0.1027	0.192 ± 0.2197
16	106.0274	1.0323	16.767 ± 0.2121	15.667 ± 0.1027	0.034 ± 0.2186
17	106.0336	0.9892	16.787 ± 0.2122	15.572 ± 0.1024	0.148 ± 0.2186
18	106.0542	1.0754	17.463 ± 0.2185	15.559 ± 0.1023	0.838 ± 0.2246
19	106.0313	1.0692	16.783 ± 0.2122	15.554 ± 0.1023	0.162 ± 0.2185
20	105.9841	1.0214	17.096 ± 0.2146	15.509 ± 0.1022	0.522 ± 0.2207
21	106.0528	1.0410	16.584 ± 0.2111	15.473 ± 0.1020	0.045 ± 0.2173
22	106.0193	1.0270	16.304 ± 0.2101	15.447 ± 0.1020	-0.209 ± 0.2163
23	106.0343	1.0663	16.540 ± 0.2109	15.423 ± 0.1019	0.050 ± 0.2171
24	105.9778	0.9913	17.114 ± 0.2147	15.423 ± 0.1019	0.625 ± 0.2208
25	106.0358	1.0662	16.608 ± 0.2112	15.416 ± 0.1019	0.126 ± 0.2174
26	106.0525	1.0444	16.579 ± 0.2111	15.407 ± 0.1018	0.107 ± 0.2172
27	106.0053	0.9881	16.662 ± 0.2115	15.399 ± 0.1018	0.197 ± 0.2176
28	106.0157	1.0514	16.487 ± 0.2107	15.396 ± 0.1018	0.025 ± 0.2168
29	106.0043	0.9921	16.697 ± 0.2117	15.395 ± 0.1018	0.236 ± 0.2178
30	105.9810	0.9939	16.951 ± 0.2134	15.384 ± 0.1018	0.501 ± 0.2194
31	105.9710	1.0659	17.103 ± 0.2146	15.378 ± 0.1017	0.660 ± 0.2206
32	105.9634	1.0453	17.115 ± 0.2147	15.367 ± 0.1017	0.683 ± 0.2207
33	105.9842	1.0098	17.045 ± 0.2141	15.365 ± 0.1017	0.614 ± 0.2201
34	105.9665	1.0210	17.170 ± 0.2153	15.343 ± 0.1016	0.761 ± 0.2212

Table 6 *continued*

Table 6 (*continued*)

<i>no.</i>	RA J2000	DEC J2000	B Magnitude	V Magnitude	BV Magnitude
35	106.0567	1.0868	16.980 ± 0.2136	15.320 ± 0.1016	0.594 ± 0.2195
36	106.0499	1.0336	16.353 ± 0.2102	15.309 ± 0.1015	-0.022 ± 0.2162
37	106.0553	1.0949	17.153 ± 0.2151	15.299 ± 0.1015	0.788 ± 0.2209
38	106.0631	1.0076	17.054 ± 0.2142	15.293 ± 0.1015	0.695 ± 0.2201
39	106.0533	1.0059	16.826 ± 0.2125	15.292 ± 0.1015	0.468 ± 0.2184
40	106.0621	1.0766	16.961 ± 0.2134	15.287 ± 0.1015	0.609 ± 0.2193
41	105.9629	1.0175	17.165 ± 0.2152	15.275 ± 0.1014	0.824 ± 0.2210
42	105.9882	1.0846	16.948 ± 0.2133	15.271 ± 0.1014	0.611 ± 0.2192
43	105.9800	1.0797	17.306 ± 0.2166	15.265 ± 0.1014	0.975 ± 0.2224
44	106.0726	1.0145	17.267 ± 0.2162	15.255 ± 0.1014	0.946 ± 0.2220
45	106.0252	1.0508	16.359 ± 0.2103	15.224 ± 0.1013	0.069 ± 0.2161
46	106.0578	1.0877	17.004 ± 0.2138	15.208 ± 0.1012	0.730 ± 0.2196
47	106.0040	1.0989	17.150 ± 0.2151	15.200 ± 0.1012	0.884 ± 0.2208
48	106.0241	1.0882	16.611 ± 0.2113	15.199 ± 0.1012	0.346 ± 0.2171
49	106.0488	1.0838	17.187 ± 0.2154	15.192 ± 0.1012	0.930 ± 0.2211
50	106.0142	1.0749	16.290 ± 0.2101	15.182 ± 0.1011	0.041 ± 0.2159
51	106.0510	1.0519	16.221 ± 0.2099	15.155 ± 0.1011	0.000 ± 0.2157
52	105.9881	1.0819	16.670 ± 0.2116	15.153 ± 0.1011	0.450 ± 0.2173
53	105.9833	1.0301	16.319 ± 0.2101	15.137 ± 0.1010	0.116 ± 0.2159
54	106.0790	1.0563	16.877 ± 0.2128	15.136 ± 0.1010	0.675 ± 0.2185
55	105.9600	1.0502	17.051 ± 0.2142	15.133 ± 0.1010	0.852 ± 0.2198
56	106.0393	0.9967	16.211 ± 0.2099	15.130 ± 0.1010	0.015 ± 0.2156
57	106.0184	1.0557	16.071 ± 0.2096	15.091 ± 0.1009	-0.087 ± 0.2153
58	105.9890	1.0160	16.734 ± 0.2119	15.082 ± 0.1009	0.585 ± 0.2176
59	106.0212	1.0846	16.200 ± 0.2098	15.080 ± 0.1009	0.054 ± 0.2155
60	106.0489	1.0496	16.100 ± 0.2097	15.072 ± 0.1009	-0.038 ± 0.2154
61	106.0272	0.9848	16.282 ± 0.2100	15.067 ± 0.1008	0.149 ± 0.2157
62	106.0359	1.0554	17.004 ± 0.2138	15.064 ± 0.1008	0.874 ± 0.2194
63	106.0579	0.9862	16.380 ± 0.2103	15.054 ± 0.1008	0.260 ± 0.2160
64	106.0080	1.0195	16.052 ± 0.2096	15.043 ± 0.1008	-0.057 ± 0.2153
65	106.0373	1.0413	15.956 ± 0.2095	15.004 ± 0.1007	-0.114 ± 0.2151
66	106.0495	1.0200	15.988 ± 0.2095	14.992 ± 0.1006	-0.070 ± 0.2151
67	106.0253	1.0730	16.233 ± 0.2099	14.991 ± 0.1006	0.177 ± 0.2155
68	106.0947	1.0782	17.212 ± 0.2157	14.969 ± 0.1006	1.177 ± 0.2211
69	106.0885	1.0511	16.815 ± 0.2124	14.959 ± 0.1006	0.790 ± 0.2179
70	105.9918	1.0284	16.011 ± 0.2096	14.949 ± 0.1005	-0.004 ± 0.2151
71	105.9795	1.0037	16.627 ± 0.2113	14.946 ± 0.1005	0.615 ± 0.2168
72	106.0498	1.1099	16.864 ± 0.2127	14.941 ± 0.1005	0.857 ± 0.2182
73	106.0286	1.0142	15.965 ± 0.2095	14.933 ± 0.1005	-0.034 ± 0.2151
74	106.0892	1.0796	16.981 ± 0.2136	14.931 ± 0.1005	0.983 ± 0.2190
75	106.0203	1.0151	15.862 ± 0.2095	14.914 ± 0.1005	-0.118 ± 0.2150

Table 6 *continued*

Table 6 (*continued*)

<i>no.</i>	RA J2000	DEC J2000	B Magnitude	V Magnitude	BV Magnitude
76	106.0427	1.0309	15.802 ± 0.2095	14.912 ± 0.1005	-0.176 ± 0.2150
77	106.0696	0.9896	16.461 ± 0.2106	14.908 ± 0.1004	0.487 ± 0.2161
78	106.0572	1.0266	15.953 ± 0.2095	14.904 ± 0.1004	-0.017 ± 0.2150
79	106.0735	1.0033	16.656 ± 0.2115	14.899 ± 0.1004	0.691 ± 0.2169
80	106.0926	0.9878	16.976 ± 0.2136	14.882 ± 0.1004	1.028 ± 0.2189
81	106.0505	1.1124	16.674 ± 0.2116	14.872 ± 0.1004	0.736 ± 0.2170
82	105.9830	1.0221	16.010 ± 0.2096	14.862 ± 0.1003	0.081 ± 0.2150
83	105.9863	1.0748	16.194 ± 0.2098	14.859 ± 0.1003	0.269 ± 0.2153
84	106.0783	1.0460	16.616 ± 0.2113	14.858 ± 0.1003	0.691 ± 0.2167
85	106.0198	1.0015	15.927 ± 0.2095	14.844 ± 0.1003	0.017 ± 0.2149
86	105.9758	1.0841	16.436 ± 0.2105	14.843 ± 0.1003	0.527 ± 0.2159
87	106.0525	1.0353	15.834 ± 0.2095	14.827 ± 0.1003	-0.059 ± 0.2149
88	105.9800	1.0532	16.493 ± 0.2107	14.825 ± 0.1003	0.602 ± 0.2161
89	106.0122	1.0208	15.883 ± 0.2095	14.824 ± 0.1002	-0.007 ± 0.2149
90	105.9896	1.0169	16.358 ± 0.2103	14.823 ± 0.1002	0.470 ± 0.2157
91	106.0998	1.0303	17.299 ± 0.2166	14.823 ± 0.1002	1.410 ± 0.2218
92	106.0106	1.0310	15.776 ± 0.2095	14.805 ± 0.1002	-0.095 ± 0.2149
93	106.0762	1.0942	16.805 ± 0.2123	14.799 ± 0.1002	0.939 ± 0.2177
94	105.9695	1.0514	16.129 ± 0.2097	14.795 ± 0.1002	0.269 ± 0.2151
95	106.0243	1.0295	15.678 ± 0.2095	14.791 ± 0.1002	-0.179 ± 0.2149
96	106.0046	1.0664	15.863 ± 0.2095	14.780 ± 0.1002	0.017 ± 0.2149
97	105.9905	1.0382	15.845 ± 0.2095	14.770 ± 0.1001	0.009 ± 0.2148
98	106.0104	1.0013	15.859 ± 0.2095	14.767 ± 0.1001	0.027 ± 0.2148
99	105.9869	0.9967	16.002 ± 0.2095	14.766 ± 0.1001	0.170 ± 0.2149
100	106.0589	1.1020	16.292 ± 0.2101	14.757 ± 0.1001	0.469 ± 0.2541
101	105.9769	1.1117	16.511 ± 0.2108	14.753 ± 0.1001	0.692 ± 0.2161
102	106.0193	1.0993	16.125 ± 0.2097	14.746 ± 0.1001	0.313 ± 0.2150
103	106.0757	0.9951	16.416 ± 0.2104	14.741 ± 0.1001	0.609 ± 0.2158
104	106.0194	1.0640	15.749 ± 0.2095	14.721 ± 0.1000	-0.038 ± 0.2148
105	106.0060	1.0872	16.234 ± 0.2099	14.673 ± 0.0999	0.494 ± 0.2152
106	106.0338	1.0576	15.639 ± 0.2096	14.668 ± 0.0999	-0.095 ± 0.2148
107	105.9565	1.0858	16.366 ± 0.2103	14.664 ± 0.0999	0.636 ± 0.2155
108	105.9657	1.1165	16.697 ± 0.2117	14.644 ± 0.0999	0.987 ± 0.2169
109	106.0116	1.0761	15.666 ± 0.2096	14.642 ± 0.0999	-0.042 ± 0.2148
110	106.0953	1.0309	16.246 ± 0.2099	14.635 ± 0.0998	0.545 ± 0.2152
111	106.0915	1.0710	16.430 ± 0.2105	14.634 ± 0.0998	0.730 ± 0.2157
112	106.0778	1.0906	16.204 ± 0.2099	14.629 ± 0.0998	0.509 ± 0.2151
113	106.0436	1.0672	15.670 ± 0.2096	14.624 ± 0.0998	-0.020 ± 0.2148
114	106.0180	1.0221	15.525 ± 0.2097	14.619 ± 0.0998	-0.160 ± 0.2149
115	106.0387	1.0906	16.355 ± 0.2102	14.612 ± 0.0998	0.677 ± 0.2154
116	105.9582	1.0737	16.554 ± 0.2110	14.596 ± 0.0998	0.892 ± 0.2162

Table 6 *continued*

Table 6 (*continued*)

<i>no.</i>	RA J2000	DEC J2000	B Magnitude	V Magnitude	BV Magnitude
117	105.9915	1.0753	15.752 ± 0.2095	14.593 ± 0.0998	0.094 ± 0.2147
118	106.0355	1.0545	15.793 ± 0.2095	14.582 ± 0.0997	0.145 ± 0.2147
119	106.0694	1.0329	15.904 ± 0.2095	14.581 ± 0.0997	0.257 ± 0.2147
120	106.0980	1.0607	16.513 ± 0.2108	14.570 ± 0.0997	0.877 ± 0.2160
121	106.0975	1.1044	16.797 ± 0.2123	14.561 ± 0.0997	1.171 ± 0.2174
122	106.0845	1.0639	15.955 ± 0.2095	14.551 ± 0.0997	0.338 ± 0.2147
123	106.0555	1.0483	15.617 ± 0.2096	14.543 ± 0.0997	0.008 ± 0.2148
124	106.0585	1.0015	15.800 ± 0.2095	14.537 ± 0.0997	0.197 ± 0.2146
125	106.0358	1.0788	15.611 ± 0.2096	14.530 ± 0.0996	0.015 ± 0.2148
126	105.9800	1.0601	15.710 ± 0.2095	14.529 ± 0.0996	0.115 ± 0.2147
127	106.0781	1.1021	16.475 ± 0.2107	14.526 ± 0.0996	0.883 ± 0.2158
128	106.0187	1.0158	15.570 ± 0.2097	14.518 ± 0.0996	-0.014 ± 0.2148
129	106.0003	0.9951	15.633 ± 0.2096	14.501 ± 0.0996	0.067 ± 0.2147
130	106.0409	1.0481	15.436 ± 0.2099	14.500 ± 0.0996	-0.130 ± 0.2150
131	106.0980	1.0964	16.628 ± 0.2113	14.474 ± 0.0995	1.088 ± 0.2164
132	106.0719	0.9990	15.835 ± 0.2095	14.469 ± 0.0995	0.299 ± 0.2146
133	106.0175	1.0704	15.448 ± 0.2099	14.463 ± 0.0995	-0.081 ± 0.2149
134	106.0884	1.0050	15.960 ± 0.2095	14.458 ± 0.0995	0.436 ± 0.2146
135	105.9741	1.0465	15.628 ± 0.2096	14.442 ± 0.0995	0.120 ± 0.2147
136	106.0433	1.1170	15.850 ± 0.2095	14.421 ± 0.0995	0.363 ± 0.2145
137	106.0517	1.1186	15.792 ± 0.2095	14.383 ± 0.0994	0.343 ± 0.2145
138	106.0503	1.1029	15.714 ± 0.2095	14.383 ± 0.0994	0.266 ± 0.2145
139	106.0129	1.0572	15.346 ± 0.2101	14.368 ± 0.0994	-0.088 ± 0.2151
140	106.0645	1.0586	15.611 ± 0.2096	14.354 ± 0.0993	0.191 ± 0.2146
141	105.9636	1.1125	16.119 ± 0.2097	14.338 ± 0.0993	0.715 ± 0.2147
142	106.0645	1.0316	15.457 ± 0.2098	14.335 ± 0.0993	0.057 ± 0.2148
143	106.0337	1.0542	15.912 ± 0.2095	14.286 ± 0.0992	0.560 ± 0.2144
144	106.0659	1.0556	15.685 ± 0.2095	14.282 ± 0.0992	0.337 ± 0.2145
145	106.0470	1.0313	15.225 ± 0.2104	14.278 ± 0.0992	-0.118 ± 0.2153
146	105.9660	1.0862	15.769 ± 0.2095	14.277 ± 0.0992	0.426 ± 0.2144
147	106.0228	1.0597	16.246 ± 0.2099	14.267 ± 0.0992	0.913 ± 0.2149
148	105.9637	1.0927	15.725 ± 0.2095	14.262 ± 0.0992	0.397 ± 0.2144
149	106.0091	1.1110	16.244 ± 0.2099	14.253 ± 0.0992	0.925 ± 0.2149
150	106.0741	1.0975	15.516 ± 0.2097	14.229 ± 0.0991	0.221 ± 0.2146
151	106.0576	1.0252	15.209 ± 0.2105	14.215 ± 0.0991	-0.073 ± 0.2153
152	106.0334	1.0417	14.215 ± 0.2152	14.203 ± 0.0991	-1.054 ± 0.2199
153	106.0514	0.9968	15.367 ± 0.2100	14.197 ± 0.0991	0.104 ± 0.2149
154	106.0524	1.1203	16.124 ± 0.2097	14.181 ± 0.0991	0.877 ± 0.2146
155	106.0752	1.0700	16.000 ± 0.2095	14.177 ± 0.0991	0.757 ± 0.2144
156	106.0431	1.0650	15.232 ± 0.2104	14.173 ± 0.0991	-0.007 ± 0.2152
157	106.0409	0.9858	15.260 ± 0.2103	14.159 ± 0.0990	0.034 ± 0.2151

Table 6 *continued*

Table 6 (*continued*)

<i>no.</i>	RA J2000	DEC J2000	B Magnitude	V Magnitude	BV Magnitude
158	106.0198	1.0527	15.772 ± 0.2095	14.152 ± 0.0990	0.554 ± 0.2143
159	106.0283	1.0747	15.206 ± 0.2105	14.145 ± 0.0990	-0.005 ± 0.2153
160	106.0535	1.0180	15.221 ± 0.2104	14.139 ± 0.0990	0.016 ± 0.2152
161	106.0385	1.0793	15.161 ± 0.2106	14.085 ± 0.0989	0.010 ± 0.2154
162	106.0024	1.0842	15.254 ± 0.2103	14.078 ± 0.0989	0.110 ± 0.2151
163	106.0465	1.0458	15.084 ± 0.2109	14.071 ± 0.0989	-0.053 ± 0.2156
164	105.9602	1.1131	15.595 ± 0.2096	14.051 ± 0.0989	0.477 ± 0.2144
165	106.0401	1.0596	15.077 ± 0.2109	14.048 ± 0.0989	-0.036 ± 0.2156
166	106.0096	0.9904	15.180 ± 0.2105	14.042 ± 0.0989	0.072 ± 0.2153
167	106.0342	1.0259	14.978 ± 0.2112	14.040 ± 0.0989	-0.128 ± 0.2160
168	105.9843	1.0058	15.159 ± 0.2106	14.017 ± 0.0988	0.076 ± 0.2153
169	106.0588	1.0190	15.894 ± 0.2095	14.014 ± 0.0988	0.814 ± 0.2142
170	106.0842	1.0595	15.297 ± 0.2102	14.001 ± 0.0988	0.230 ± 0.2149
171	106.0761	1.0389	15.148 ± 0.2106	13.993 ± 0.0988	0.089 ± 0.2154
172	105.9799	1.0022	15.113 ± 0.2108	13.989 ± 0.0988	0.058 ± 0.2155
173	106.0738	1.0686	15.215 ± 0.2104	13.969 ± 0.0988	0.181 ± 0.2151
174	106.0007	1.0140	14.970 ± 0.2113	13.963 ± 0.0988	-0.059 ± 0.2160
175	106.0907	1.0583	15.422 ± 0.2099	13.904 ± 0.0987	0.452 ± 0.2146
176	106.0041	1.0138	15.230 ± 0.2104	13.902 ± 0.0987	0.261 ± 0.2151
177	105.9887	1.0022	14.982 ± 0.2112	13.898 ± 0.0987	0.019 ± 0.2159
178	106.0584	1.0184	15.389 ± 0.2100	13.897 ± 0.0987	0.426 ± 0.2147
179	106.0181	1.0145	14.893 ± 0.2116	13.886 ± 0.0987	-0.058 ± 0.2162
180	105.9647	1.1025	15.268 ± 0.2103	13.879 ± 0.0987	0.323 ± 0.2149
181	106.0678	1.0223	15.613 ± 0.2096	13.868 ± 0.0986	0.679 ± 0.2143
182	105.9682	1.0181	14.993 ± 0.2112	13.857 ± 0.0986	0.069 ± 0.2158
183	106.0331	1.0331	14.787 ± 0.2120	13.822 ± 0.0986	-0.101 ± 0.2166
184	105.9976	1.0363	14.834 ± 0.2118	13.814 ± 0.0986	-0.046 ± 0.2164
185	106.0240	1.1174	15.046 ± 0.2110	13.794 ± 0.0985	0.186 ± 0.2156
186	106.0583	1.0340	14.768 ± 0.2121	13.769 ± 0.0985	-0.067 ± 0.2167
187	106.0455	1.0493	14.770 ± 0.2121	13.759 ± 0.0985	-0.055 ± 0.2167
188	106.0000	1.0750	14.826 ± 0.2119	13.745 ± 0.0985	0.015 ± 0.2164
189	105.9948	1.0968	14.911 ± 0.2115	13.723 ± 0.0985	0.122 ± 0.2161
190	106.0439	1.0398	14.733 ± 0.2123	13.706 ± 0.0984	-0.039 ± 0.2168
191	106.0677	1.0189	14.936 ± 0.2114	13.705 ± 0.0984	0.165 ± 0.2159
192	105.9917	1.0253	14.765 ± 0.2121	13.689 ± 0.0984	0.010 ± 0.2167
193	106.0773	1.0171	14.846 ± 0.2118	13.671 ± 0.0984	0.109 ± 0.2163
194	106.0129	1.0222	14.678 ± 0.2126	13.657 ± 0.0984	-0.046 ± 0.2171
195	106.0043	1.0295	14.678 ± 0.2126	13.651 ± 0.0984	-0.039 ± 0.2171
196	106.0304	1.0291	14.696 ± 0.2125	13.646 ± 0.0984	-0.016 ± 0.2170
197	106.0350	1.0280	14.538 ± 0.2133	13.638 ± 0.0984	-0.166 ± 0.2177
198	106.0388	1.1202	15.064 ± 0.2109	13.628 ± 0.0984	0.370 ± 0.2154

Table 6 *continued*

Table 6 (*continued*)

<i>no.</i>	RA J2000	DEC J2000	B Magnitude	V Magnitude	BV Magnitude
199	106.0456	0.9960	14.748 ± 0.2122	13.612 ± 0.0983	0.069 ± 0.2167
200	106.0485	1.0860	16.056 ± 0.2096	13.580 ± 0.0983	1.409 ± 0.2141
201	106.0764	0.9984	14.729 ± 0.2123	13.556 ± 0.0983	0.106 ± 0.2168
202	106.0223	1.0604	14.671 ± 0.2126	13.548 ± 0.0983	0.057 ± 0.2170
203	105.9938	1.0694	14.602 ± 0.2129	13.532 ± 0.0983	0.004 ± 0.2174
204	106.0321	1.0136	14.535 ± 0.2133	13.492 ± 0.0982	-0.023 ± 0.2177
205	106.0443	1.0383	14.500 ± 0.2135	13.482 ± 0.0982	-0.048 ± 0.2179
206	106.0882	1.0696	14.796 ± 0.2120	13.454 ± 0.0982	0.276 ± 0.2164
207	106.0641	1.0832	14.568 ± 0.2131	13.439 ± 0.0982	0.063 ± 0.2175
208	106.0291	1.0333	14.415 ± 0.2140	13.428 ± 0.0982	-0.079 ± 0.2183
209	106.0229	1.0266	14.448 ± 0.2138	13.417 ± 0.0982	-0.035 ± 0.2181
210	106.0020	1.0358	14.424 ± 0.2139	13.358 ± 0.0981	0.000 ± 0.2182
211	106.0593	1.0050	14.422 ± 0.2139	13.260 ± 0.0980	0.096 ± 0.2182
212	106.0706	1.1025	14.610 ± 0.2129	13.235 ± 0.0980	0.310 ± 0.2172
213	106.0496	1.0402	14.225 ± 0.2151	13.233 ± 0.0980	-0.074 ± 0.2194
214	106.0169	1.0001	14.281 ± 0.2147	13.228 ± 0.0980	-0.013 ± 0.2190
215	105.9710	1.0889	14.416 ± 0.2139	13.180 ± 0.0980	0.170 ± 0.2182
216	105.9817	1.1130	14.408 ± 0.2140	13.164 ± 0.0979	0.178 ± 0.2183
217	106.0095	1.0843	14.253 ± 0.2149	13.129 ± 0.0979	0.057 ± 0.2192
218	106.0470	1.0873	14.245 ± 0.2150	13.043 ± 0.0979	0.135 ± 0.2192
219	106.0530	1.0459	14.185 ± 0.2153	13.033 ± 0.0978	0.086 ± 0.2195
220	105.9752	1.1037	14.521 ± 0.2134	13.022 ± 0.0978	0.434 ± 0.2176
221	106.0302	1.0893	14.981 ± 0.2112	12.948 ± 0.0978	0.967 ± 0.2155
222	106.0501	1.0747	14.205 ± 0.2152	12.932 ± 0.0978	0.207 ± 0.2194
223	106.0682	1.0232	14.178 ± 0.2154	12.923 ± 0.0978	0.188 ± 0.2196
224	106.0939	1.1049	14.700 ± 0.2124	12.880 ± 0.0977	0.754 ± 0.2167
225	106.0450	1.0694	13.967 ± 0.2168	12.855 ± 0.0977	0.045 ± 0.2209
226	106.0719	1.0437	13.962 ± 0.2168	12.826 ± 0.0977	0.069 ± 0.2209
227	106.0484	1.0869	14.093 ± 0.2159	12.804 ± 0.0977	0.224 ± 0.2201
228	106.0237	1.0703	13.903 ± 0.2172	12.782 ± 0.0977	0.054 ± 0.2213
229	106.0564	1.0346	14.443 ± 0.2138	12.780 ± 0.0977	0.598 ± 0.2179
230	106.0243	1.0098	14.401 ± 0.2140	12.779 ± 0.0977	0.556 ± 0.2182
231	106.0213	1.0483	13.877 ± 0.2174	12.756 ± 0.0977	0.055 ± 0.2215
232	106.0221	1.0498	14.312 ± 0.2146	12.620 ± 0.0976	0.626 ± 0.2187
233	106.0979	0.9930	13.864 ± 0.2175	12.610 ± 0.0976	0.188 ± 0.2216
234	106.0155	1.0043	14.250 ± 0.2149	12.585 ± 0.0976	0.599 ± 0.2190
235	106.0294	1.0663	13.773 ± 0.2182	12.579 ± 0.0976	0.128 ± 0.2222
236	106.0385	1.0540	13.705 ± 0.2187	12.529 ± 0.0975	0.110 ± 0.2227
237	105.9645	1.0739	13.698 ± 0.2187	12.514 ± 0.0975	0.118 ± 0.2227
238	106.0665	1.0144	13.736 ± 0.2185	12.505 ± 0.0975	0.165 ± 0.2225
239	106.0648	1.0807	13.682 ± 0.2189	12.495 ± 0.0975	0.121 ± 0.2229

Table 6 *continued*

Table 6 (*continued*)

<i>no.</i>	RA J2000	DEC J2000	B Magnitude	V Magnitude	BV Magnitude
240	106.0614	1.0185	14.168 ± 0.2155	12.446 ± 0.0975	0.656 ± 0.2195
241	106.0046	1.1011	14.186 ± 0.2153	12.445 ± 0.0975	0.675 ± 0.2194
242	106.0342	1.0884	14.151 ± 0.2156	12.413 ± 0.0975	0.673 ± 0.2196
243	106.0104	1.0195	13.443 ± 0.2207	12.381 ± 0.0975	-0.004 ± 0.2247
244	105.9915	1.0714	14.050 ± 0.2162	12.311 ± 0.0974	0.674 ± 0.2202
245	105.9882	1.0872	13.186 ± 0.2229	12.028 ± 0.0973	0.092 ± 0.2267
246	105.9898	1.0247	13.183 ± 0.2229	11.917 ± 0.0973	0.201 ± 0.2267
247	105.9651	1.1109	13.741 ± 0.2184	11.812 ± 0.0973	0.863 ± 0.2223
248	106.0157	1.0393	13.167 ± 0.2230	11.787 ± 0.0973	0.314 ± 0.2268
249	105.9571	1.0948	13.300 ± 0.2219	11.776 ± 0.0973	0.458 ± 0.2257
250	106.0672	1.0204	13.436 ± 0.2208	11.528 ± 0.0972	0.842 ± 0.2246
251	106.0140	1.0670	10.760 ± 0.2476	9.315 ± 0.0971	0.380 ± 0.2510

NOTE—